pISSN 1229-3008 eISSN 2287-6251
Progress in Superconductivity and Cryogenics
Vol.21, No.1, (2019), pp.18~24 https://doi.org/10.9714/psac.2019.21.1.018

Effect of boron milling on phase formation and critical current density of MgB_2 bulk superconductors

M. O. Kang[a,b], J. Joo[b], B.–H. Jun[a], S.-D. Park[a], C. S. Kim[c], and C.-J. Kim[*,a]

[a] *Korea Atomic Energy Research Institute, Daejeon, Korea*
[b] *Sungkyunkwan University, Suwon, Korea*
[c] *Korea Research Institute of Standards and Science, Daejeon, Korea*

(Received 14 March 2019; revised or reviewed 27 March 2019; accepted 28 March 2019)

Abstract

This study was carried out to investigate the effect of milling of boron (B), which is one of raw materials of MgB_2, on the critical current density (J_c) of MgB_2. B powder used in this study is semi-amorphous B (Pavezyum, Turkey, 97% purity, 1 micron). The size of B powder was reduced by planetary milling using ZrO_2 balls (a diameter of 2 mm). The B powder and balls with a ratio of 1:20 were charged in a ceramic jar and then the jar was filled with toluene. The milling time was varied from 0 to 8 h. The milled B powders were mixed with Mg powder in the composition of (Mg+2B), and the powder mixtures were uniaxially pressed at 3 tons. The powder compacts were heat-treated at 700℃ for 1 h in flowing argon gas. Powder X-ray diffraction and FWHM (Full width at half maximum) were used to analyze the phase formation and crystallinity of MgB_2. The superconducting transition temperature (T_c) and J_c of MgB_2 were measured using a magnetic property measurement system (MPMS). It was found that B_2O_3 was formed by B milling and the subsequent drying process, and the volume fraction of B_2O_3 increased as milling time increased. The T_c of MgB_2 decreased with increasing milling time, which was explained in terms of the decreased volume fraction of MgB_2, the line broadening of MgB_2 peaks and the formation of B_2O_3. The J_c at 5 K increased with increasing milling time. The J_c increase is more remarkable at the magnetic field higher than 3 T. The J_c at 5 K and 4 T was the highest as 4.37×10^4 A/cm^2 when milling time was 2 h. The J_c at 20 K also increased with increasing milling time. However, The J_c of the samples with the prolonged milling for 6 and 8 h were lower than that of the non-milled sample.

Keywords: MgB_2, ball milling, B_2O_3, superconducting properties, FWHM

1. INTRODUCTION

Superconductors that show zero resistivity at the critical transition temperature (T_c) can be used in medical, transportation, communication and power applications [1-2]. The MgB_2 has a high T_c of 39 K [3], so it can be cooled by cooler without using expensive liquid helium if the superconducting equipment is made using MgB_2.

The MgB_2 has the coherence length of 5.2 nm [4], which is longer than that of the high-temperature oxide superconductor [2]. The current anisotropy of MgB_2 is about 2-3, that is much lower than that of the oxide superconductor [5].

It is necessary to lower the price and increase the critical current density (J_c) to produce highly efficient and practically available superconducting wires. The MgB_2 is considered as a next-generation superconducting wire which can replace the conventional NbTi wire because of the high T_c, low cost and simple fabrication process.

The *in-situ* process is one of the most widely used methods for the synthesis of MgB_2 superconductor [6-7]. The quality of precursor powder is an important variable affecting the superconductivity. The particle size, connectivity of grain and purity of the raw powders have a significant effect on the J_c of MgB_2 [8-10]. Therefore, the powder quality required for the process should be carefully controlled.

The synthesizing process for MgB_2 is simple because it can be manufactured by the powder reaction process [7, 11-12]. However, the J_c of MgB_2 at high magnetic fields is low [13], which make it difficult to use MgB_2 in high field applications. The J_c of MgB_2 is affected by grain size, defects, chemical doping and lattice distortion [8, 14-18]. The grain boundaries of MgB_2 act as a flux pinning center, which improves J_c in the magnetic field. If the size of grains is refined, the number of grain boundaries increases [19].

Mechanical milling of boron (B) has been applied to reduce the grain size of MgB_2 [19-21]. The grain size of the *in-situ* processed MgB_2 using Mg and B powders is influenced by the size of B. This is because the diffusion of B is relatively slow compared to Mg and thus MgB_2 is nucleated at the B powder. The melting point (m. p.) of Mg is low (650℃) [22], so diffusion occurs rapidly at the heat treatment temperature. When heat treatment is performed at a temperature higher than the m. p. of Mg, the Mg melts. It is necessary to reduce the particle size of the B powder to obtain the fine grain size of MgB_2.

The purpose of this study is to investigate the effect of B particle size on the J_c of MgB_2. The size of B powder was reduced by ball milling and milling time was varied. The inexpensive, low purity and micro-sized B powder was

* Corresponding author: cjkim2@kaeri.re.kr

used to establish the development of a cost-effective process. The MgB_2 was synthesized by the powder reaction process using the non-milled and milled B powders with various milling times. The effect of the B size on the apparent density, phase formation, T_c and J_c were examined.

2. EXPERIMENTAL PROCEDURE

2.1. Ball milling

Spherical Mg (99.9% purity, average size 27.5 μm, Hana AMT, Korea) and plate-shaped B (95~97% purity, average size 1 μm, Pavezyum, Turkey) powders were used as raw powders to synthesize MgB_2. As can be seen Fig. 1(a), small and large plate-like B powders are observed in the form of agglomeration. The Mg powder is semi-spherical in shape (Fig. 1(b)).

The planetary milling was used to reduce the particle size of B powder. The B powder and ZrO_2 balls with a diameter 2 mm were weighed to a ratio of 1:20 and put in a ceramic jar for milling B powder. Toluene was used as a solvent. The planetary milling machine rotated at a speed of 200 rpm for 0, 2, 4, 6 and 8 h. After milling, the balls were separated from the (B+toluene) solution by using a sieve and were washed with toluene. The milled B powder was dried at 120℃ for 20 h in a vacuum for removing toluene.

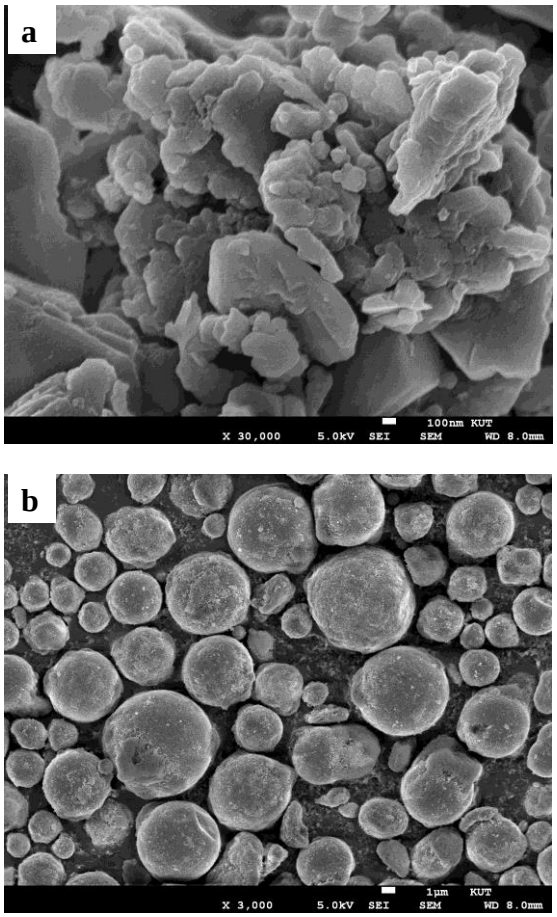

Fig. 1. FE-SEM image of (a) B and (b) Mg powders used as raw materials.

2.2. Synthesis of MgB_2

The milled B powders were mixed to a ratio of Mg:B = 1:2. The powders were mixed thoroughly using a mortar and pestle by hand for 30 minutes. The mixed powders were put in a steel mold with a diameter of 10 mm and uniaxially pressed at a pressure of 3 tons into pellets. The pellets were put in a Ti tube and the Ti tube was sealed to prevent Mg oxidation during heat treatment. And then the pellets were heated at 700℃ at a rate of 5℃/min in flowing Ar gas and maintained at this temperature for 1 h. Since m. p. of Mg is 650℃, MgB_2 is formed by the reaction of eq. (1) when the pellet is heat-treated above the m. p.. Where *l* and *s* denote a liquid and solid, respectively.

$$Mg\,(l) + 2B\,(s) \rightarrow MgB_2\,(s) \tag{1}$$

2.3. Measurement of properties

The size of the non-milled and the milled powders were investigated using a field emission scanning electron microscope (FE-SEM).

The apparent density of pellets of before/after heat treatment was measured using the data of a volume and weight of the pellets.

The heat-treated MgB_2 bulk samples were crushed into powders and the powder samples were used to analyze the phase formation after the heat treatment, the volume fraction of MgB_2 and its grain size. The formed phases were identified from the X-ray diffraction patterns of the heat-treated samples. The volume fractions of MgB_2, MgO and other residual phases were calculated using eq. (2).

$$F(MgB_2) = \frac{\sum I_{MgB_2}}{\sum I_{MgB_2} + \sum I_{Mg} + \sum I_{MgO}} \times 100 \tag{2}$$

The volume fraction, *F* of MgB_2 was calculated from the intensities of diffraction peaks of MgB_2, Mg and MgO.

The heat-treated samples were cut into a dimension of $3\times2\times1$ mm^3 using a diamond saw and the cut samples were used to estimate T_c and J_c at the magnetic field. The magnetic moment–temperature (*M*-*T*) and magnetic moment–magnetic field (*M*-*B*) of the samples were measured using a MPMS (Magnetic Property Measurement System) with a maximum magnetic field of 5 Tesla. The J_c at 5 K and 20 K were calculated using an extended Bean's critical model [23] of eq. (3).

$$J_c = 20\Delta M / a(1 - 3a/b) \tag{3}$$

Where ΔM is the magnetization difference (M_decreasing field region - M_increasing field region) at a constant magnetic field, and *a* and *b* are dimension parameters regarding the sample dimensions.

3. RESULTS AND DISCUSSION

Figs. 2(a)-(d) show the FE-SEM images of milled B powders. In the milled powders, small crushed B particles

are observed with the large particles. The number of the crushed powders increases as milling time increases, resulting in the decrease in an average particle size of B. As milling time exceeds 6 h, almost all particles appear to be crushed into smaller ones, so the particle distribution becomes uniform.

Fig. 3 shows X-ray diffraction patterns of the B powders milled for 0 to 8 h. In the non-milled B powder, many diffraction lines were observed from $2\theta = 10^\circ$ to 80°, which means that the B powder is crystalline. The peak intensity of the diffraction lines decreased with increasing milling time and the peak became broader (line broadening). The line broadening is thought to be caused by the grain size refinement [24] of the B powders by mechanical milling. Moreover, the peaks of B_2O_3 were observed at $2\theta = 14.6^\circ$ and 28° (marked by * in Fig. 3) and their intensities were strengthened as milling time increased. B_2O_3 is seemed to be formed by the oxidation of B of eq. (4) during the drying process performed after milling. The increment of the volume fraction of B_2O_3 with milling time is attributed to the increased surface area of the B powders.

$$B\,(s) + O_2\,(g) \rightarrow B_2O_3\,(s) \qquad (4)$$

Fig. 4 shows the variation of an apparent density as a function of milling time. We calculated the density of the pellets before and after heat treatment by measuring the diameter, thickness and weight of pellets. Pores (open pore + closed pore) are included in samples. The density of the pellet pressed using the non-milled B powder is 1.49 g/cm^3. The density increases proportionally with milling time and reaches 1.73 g/cm^3 when milling time is 8 h. Under the applied pressures of this experiment, the smaller the size of B powder is, the higher the density is. The density of the compacted pellets influenced a density of the samples after the heat treatment. The density of non-milled sample is 1.32 g/cm^3, and it increases to 1.50 g/cm^3 when milling time is 8 h.

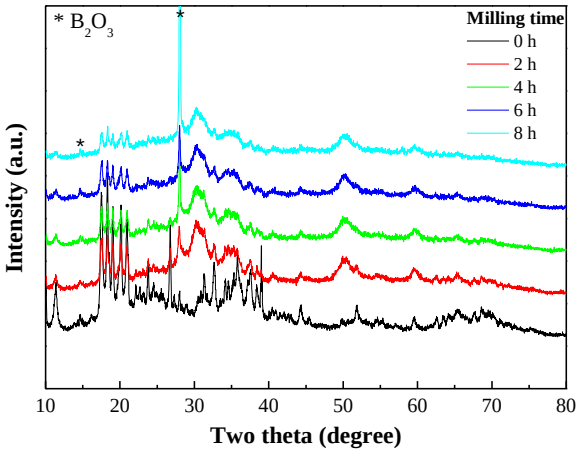

Fig. 3. Variation of X-ray diffraction patterns of the B powders as a function of milling time.

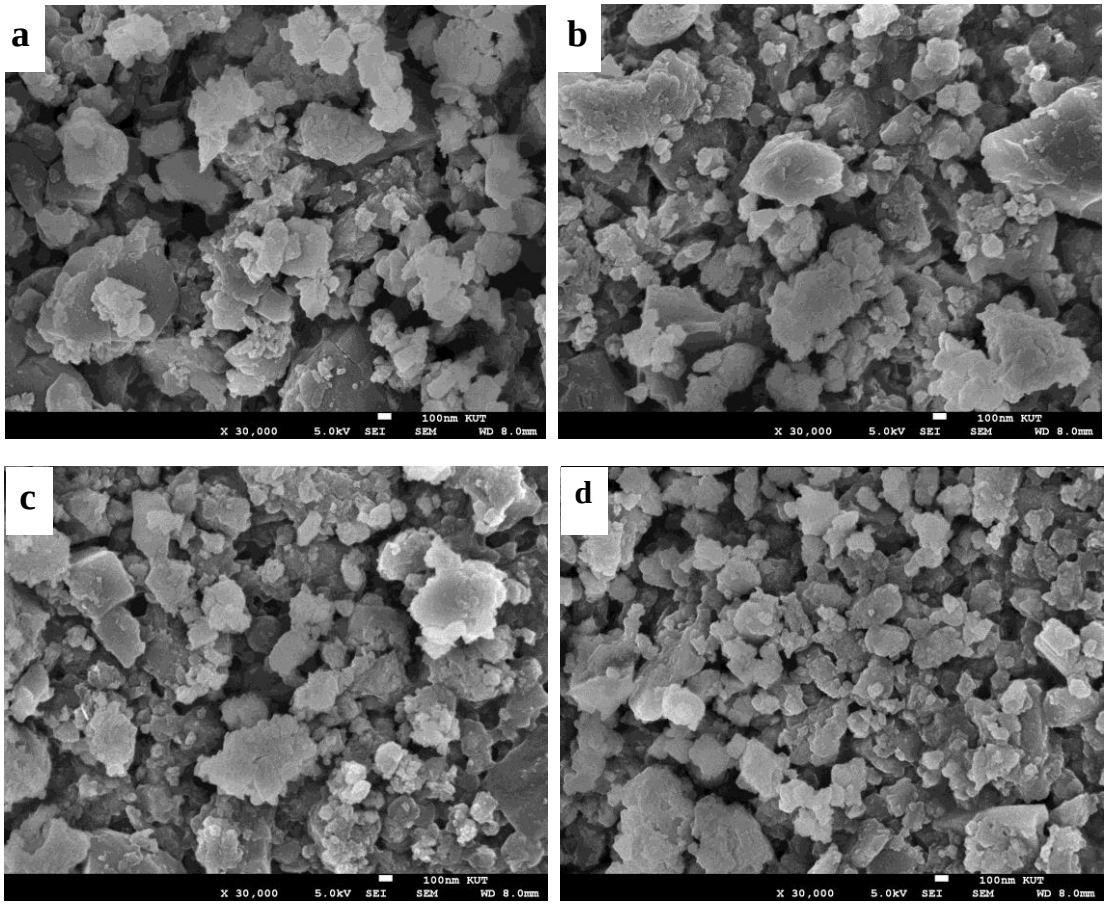

Fig. 2. FE-SEM images of the B powders milled for (a) 2 h, (b) 4 h, (c) 6 h, and (d) 8 h.

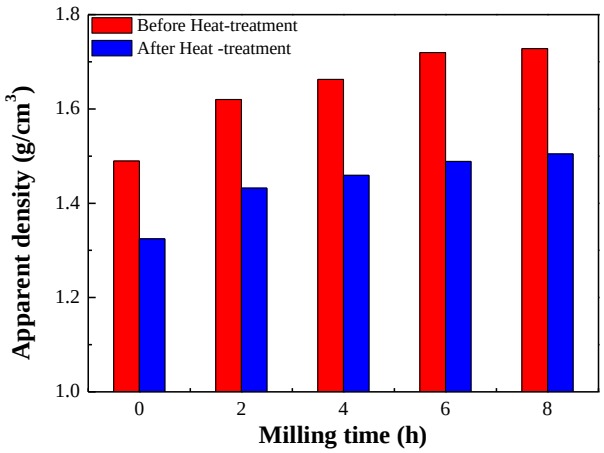

Fig. 4. Histogram of an apparent density before/after the heat treatment as a function of milling time.

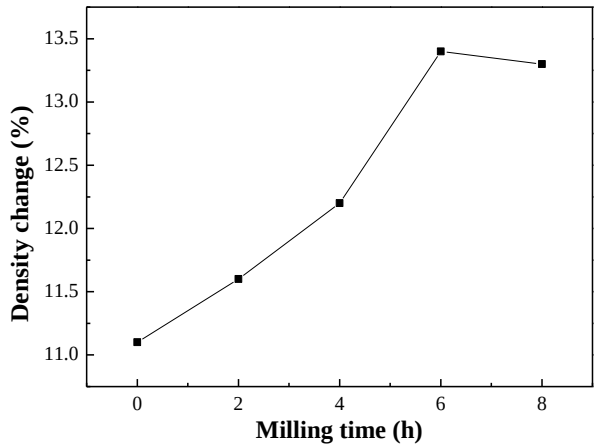

Fig. 5. Variation of an apparent density of the heat-treated sample as a function of milling time.

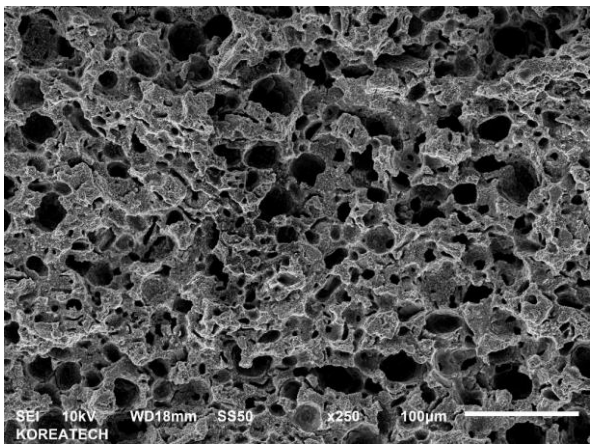

Fig. 6. SEM micrograph of the MgB_2 sample after heat treatment.

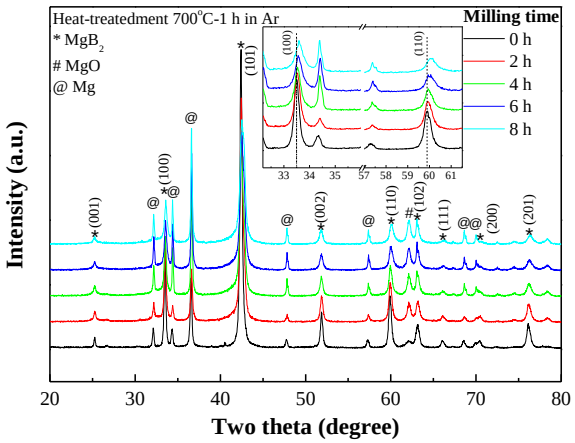

Fig. 7. Powder X-ray diffraction patterns of the samples heat-treated using the non-milled and milled B powders.

From the data of Fig. 4, the % density change (the difference in density before/after heat treatment) of pellets was calculated as a function of milling time and the result is shown in Fig. 5. The density change increases linearly when milling time increases to 6 h. However, the density change of the sample using milled B powder for 8 h is slightly less than 6 h.

The feature that should be noted in this study is the decrease of the apparent density after heat treatment regardless of milling time. As seen in Fig. 4 and 5, the density of all samples decreased after the heat treatment. A similar result has been published in several previous papers [7, 25]. The causes of the density decrease are the increase of a volume of samples after heat treatment and the formation of pores in samples. During the heat treatment, MgB_2 is formed following eq. (1). Many pores are formed because Mg powder melted and the sites where Mg powder existed were changed into pores. Therefore, the shape of the pores is analogue to that of Mg powder used (see Fig. 6). In addition to the formation of pores, the outgrowth of MgB_2 plates, which results in the pellet expansion [26], affected the decrease in the apparent density.

Fig. 7 shows the XRD patterns of MgB_2 prepared using the non-milled and milled B powders for 2 to 8 h. The major formed phase in samples is MgB_2. The peaks of the non-reacted Mg and MgO that were formed by oxidation of Mg were also observed in diffraction patterns. The formation of MgO seems to be related to the B_2O_3 observed in the milled B powder. A larger amount of B_2O_3 existed in the milled B powder compared to that of the non-milled B powder. The m. p. of B_2O_3 is 450˚C [27]. The B_2O_3 melts at 700˚C, which is the heat treatment temperature, and oxygen of B_2O_3 might react with Mg to form MgO [27-28]. The cause of the presence of the residual Mg in samples using the milled B powders is unclear and further research is needed to clarify it.

Another interesting feature of this result is the shift of the MgB_2 (hkl) diffraction lines of the samples using the milled B powders. As shown in the small box at the top of Fig. 7, the (100) and (110) peaks of MgB_2 shift to the right from their original positions as milling time increases. In Bragg's law, the shift of 2θ means the change of the lattice parameters. Other studies for MgB_2 prepared using the milled B powders also has been showed a similar result to this study. The use of milled B caused the lattice distortion of MgB_2 (the line broadening) and changed the lattice parameters (the 2θ shift) of MgB_2. The C from toluene [21] or ZrO_2 balls [29], which were used as a solvent and milling

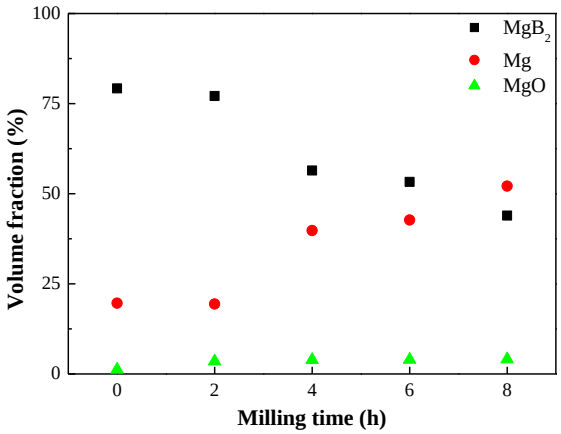

Fig. 8. Volume fraction of MgB_2, Mg and MgO as a function of milling time.

medium, respectively, appear to be incorporated with MgB_2 lattices.

The volume fraction of the phases formed in the heat-treated samples is shown in Fig. 8. The volume fraction of MgB_2 of the sample using the non-milled B powder is about 75%. The volume fraction of MgB_2 in the sample using 2 h milled B powder is similar to that using the non-milled B powder. However, it decreases as milling time increases further, which was caused by the presence of unreacted Mg and the formation of MgO. When B powder is milled, the particle size of powder becomes smaller, so that the surface area per unit volume and the reactivity increases [30]. It induces the formation of B_2O_3 that was observed in Fig. 3. The formation of B_2O_3 seems not only to promote the formation of MgO during heat treatment but also to suppress the formation of MgB_2.

The grain size and microstrain of MgB_2 were calculated from FWHM (Full width at half maximum) of diffraction lines of MgB_2 of Fig. 7 using eq. (5) [31].

$$G(t) = 0.9\lambda/B\cos\theta \quad (5)$$

Where $G(t)$ is the grain size of MgB_2, λ is the wavelength of X-ray target, B is the half width of peaks and θ is the angle of an incident beam. The FWHM, grain size and microstrain of MgB_2 calculated were summarized in TABLE I. The FWHM of (002) peak is 0.238 for the MgB_2 prepared using the non-milled B powder. As milling time increased to 2, 4, 6 and 8 h, FWHM also increased to 0.293, 0.372, 0.369 and 0.440. FWHM of the (110) peak shows a similar tendency to that of the (002) peak. It indicates that atoms arrangement in MgB_2 was displaced from the original lattice positions when using the milled B powders. The distortion of the B lattice seems to affect the crystallinity of MgB_2 because MgB_2 grains is nucleated at B particles.

As shown in TABLE 1, the grain sizes of MgB_2 were 90.6 nm, 73.3 nm, 49.7 nm and 49.7 nm, respectively for 0, 2, 4 and 6 h. It because when milling time was increased, the B particles became fine and a larger number of MgB_2 were nucleated at the B particles. The grain size of MgB_2 is proportionally decreased with increasing milling time but it

TABLE I
FWHM OF (002) AND (110) PEAK AND CALCULATED GRAIN SIZE AND MICROSTRAIN AS A FUNCTION OF MILLING TIME.

Milling time (h)	FWHM		Grain size (nm)	Microstrain (%)
	(002)	(110)		
0	0.238	0.285	90.6	0.15
2	0.293	0.342	73.3	0.17
4	0.372	0.417	49.7	0.17
6	0.369	0.482	49.7	0.19
8	0.440	0.440	64.2	0.32

increases to 64.2 nm as milling time increases further to 8 h. At this moment, the cause for that is unclear. One possible cause is the formation of an agglomeration of the fine B powders or the contamination of the B powder with impurity elements from the processing environment. The prolonged milling might cause the B powder to become very fine and have a large specific surface area, which forms the agglomeration. Further study is needed to clarify it and establish the optimum condition of milling.

Fig. 9 shows the normalized *M-T* curves of the MgB_2 samples prepared using the non-milled and milled B powders. The $T_{c,onset}$ of the sample prepared with non-milled B powder is as high as 37.5 K. As milling time increased to 2, 4, 6 and 8 h, $T_{c,onset}$ decreased to 37 K, 36.5 K, 35.5 K and 33.5 K. This result can be explained in term of the decreased volume fraction of MgB_2 and the increased values of FWHM with increasing milling time, which were observed in the XRD analysis of Fig. 8 and Table I.

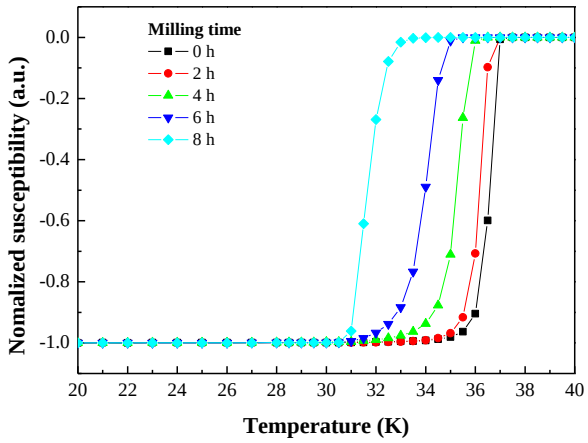

Fig. 9. *M-T* curves of MgB_2 prepared using non-milled and milled B powders.

TABLE II
SUPERCONDUCTING TRANSITION TEMPERATURES AND TRANSITION WIDTH OF THE SAMPLES PREPARED USING THE NON-MILLED AND MILLED POWDER.

Milling time (h)	0	2	4	6	8
$T_{c,onset}$ (K)	37.5	37.0	36.5	35.5	33.5
$T_{c,mid}$ (K)	36.6	36.3	35.3	34.1	32.0
ΔT_c (K)	0.9	0.7	1.2	1.4	1.5

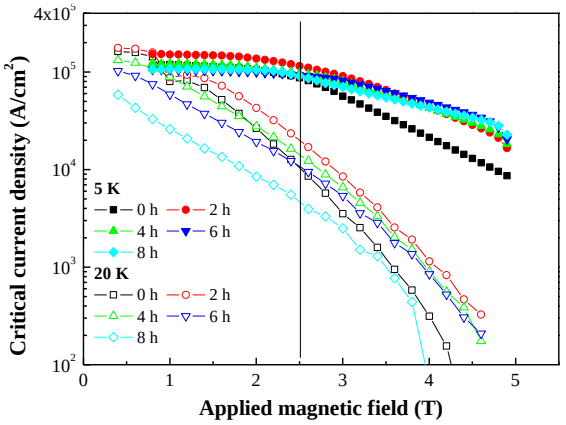

Fig. 10. J_c-B curves at 5 K and 20 K of MgB_2 prepared using non-milled and milled B powders.

The superconducting transition width (ΔT_c) increases linearly from 0.9 K to 1.5 K as milling time increases from 0 h to 8 h. When a large volume of a superconducting phase of a good quality is formed in samples, the slope of the M-T curve is steep and the width of ΔT_c becomes narrow. This can also be explained by the X-ray analysis for the volume fraction and microstrain of the formed MgB_2 phases. The effects of milling time on the superconducting transition temperatures are summarized in TABLE II.

Fig. 10 shows the J_c-B curves at 5 K and 20 K of the samples prepared using non-milled and milled B powders. For the 5 K curves, the J_c decreased as the magnetic field increased because the magnetic field interferes with the flow of superconducting current. The sample prepared using 2 h milled powder (marked by red closed circles) shows the highest J_c up to 2.5 T. As the magnetic field increased further, the J_c became slightly lower or similar to those of other samples.

The sample prepared using non-milled B powder shows the lowest J_c at the high magnetic fields above 2.5 T. As can be seen in the X-ray analysis when milled B was used, the volume fraction and the grain of MgB_2 decreased and microstrain increased. This indicates that in spite of the reduced volume fraction of the superconducting phase, the grain boundaries and the lattice distortion play a role in increasing J_c at the magnetic fields.

The J_c–B curves at 20 K show similar result to that at 5 K (the highest J_c for 2 h). J_c of samples using the B powder milled for 4 and 6 h is higher than that for 0 h. However, J_c decreased as milling time increased further to 8 h. This is because the formation of B_2O_3 was enhanced, which induced the oxidation of Mg and suppressed the MgB_2 phase formation. This result indicates that there is an optimum milling time to maximize the milling effect.

The J_c at 5 K and 2 T for 2 h is 1.38×10^5 A/cm^2 and the J_c at 5 K and 4 T for 6 h is 4.86×10^4 A/cm^2. The J_c at 20 K is also the highest for 2 h (4.30×10^4 A/cm^2 at 2 T and 1.17×10^4 A/cm^2 at 4 T).

3. CONCLUSIONS

The milling effect of B powder on the J_c of MgB_2 was studied. B_2O_3 was formed during the milling and drying process, and its amount was proportional to milling time. The presence of B_2O_3 induced the formation of MgO and suppressed the formation of MgB_2. The grain size of MgB_2 was reduced by the B milling and the microstrain in MgB_2 lattice was increased. The use of the milled B powder decreased the T_c of MgB_2 by reducing the volume fraction of MgB_2 and increasing the lattice distortion. In spite of the reduce volume fraction of MgB_2 by using of the milled B powder, the J_c was enhanced due to the presence of the large number of grain boundaries and the lattice strain. In this study, the optimum milling time to obtain the high J_c was 2 h.

ACKNOWLEDGMENT

This research was financially supported by the Ministry of SMEs and Startups (MSS), Korea, under the “Regional Specialized Industry Development Program (R0004502)” supervised by the Korea Institute for Advancement of Technology (KIAT).

REFERENCES

[1] W. V. Hassenzahl, D. W. Hazelton, B. K. Johnson, P. Komarek, M. Noe and C. T. Reis, “Electric power applications of superconductivity,” *Proceedings of The IEEE*, vol. 92, no. 10, pp. 1655-1674, 2004.

[2] D. Larbalestier, A. Gurevich, D. M. Feldmann and A. Polyanskii, “High-T_c superconducting materials for electric power applications,” *Nature*, vol. 414, pp. 368-377, 2001.

[3] J. Nagamatsu, N. Nakagawa, T. Muranaka, Y. Zenitani and J. Akimitsu, “Superconductivity at 39 K in magnesium diboride,” *Nature*, vol. 410, pp. 63-64, 2001.

[4] D. K. Finnemore, J. E. Ostenson, S. L. Bud’ko, G. Lapertot and P. C. Canfield, “Thermodynamic and transport properties of superconducting $Mg^{10}B_2$,” *Phys. Rev. Lett.*, vol. 86, pp. 2420-2422, 2001.

[5] Y. Eltsev, S. Lee, K. Nakao, N. Chikumoto, S. Tajima, N. Koshizuka and M. Murakami, “Anisotropic superconducting properties of MgB_2 single crystals probed by in-plane electrical transport measurements,” *Phys. Rev. B.*, vol. 65, pp. 140501, 2002.

[6] W. Goldacker, S. I. Schlachter, B. Obst and M. Eisterer, “*In situ* MgB_2 round wires with improved properties,” *Supercond. Sci. Technol.*, vol. 17, pp. S490-S495, 2004.

[7] C. -J. Kim, J. H. Yi, B. -H. Jun, B. Y. You, S. -D. Park and K. -N. Choo, “Reaction-induced pore formation and superconductivity in *in situ* processed MgB_2 superconductors,” *Physica C*, vol. 502, pp. 4-9, 2014.

[8] D. Wang, Y. Ma, Z. Yu, Z. Gao, X. Zhang, K. Watanabe and E. Mossang, “Strong influence of precursor powder on the critical current density of Fe-sheathed MgB_2 tapes,” *Supercond. Sci. Technol.*, vol. 20, pp. 574-578, 2007.

[9] A. Serquis, X. Z. Liao, Y. T. Zhu, J. Y. Coulter, J. Y. Huang, J. O. Willis, D. E. Peterson and F. M. Mueller, “Influence of microstructures and crystalline defects on the superconductivity of MgB_2,” *J. Appl. Phys.*, vol. 92, pp. 351-356, 2002.

[10] P. Kováč, B. Birajdar, I. Hušek, T. Holúbek and O. Eibl, “Stabilized *in situ* rectangular MgB_2 wires: the effect of B purity and sheath materials,” *Supercond. Sci. Technol.*, vol. 21, pp. 045011, 2008.

[11] Q. Z. Shi, Y. C. Liu, Q. Zhao and Z. Q. Ma, “Phase formation process of bulk MgB_2 analyzed by differential thermal analysis during sintering,” *J. Alloys compd.*, vol. 458, pp. 553-557, 2008.

[12] M. Muralidhar, A. Ishihara, K. Suzuki, Y. Fukumoto, Y. Yamamoto and M. Tomita, "Optimization of the fabrication process for high trapped field MgB_2 bulks," *Physica C*, vol. 494, pp. 85-88, 2013.

[13] M. Muralidhar, N. Kenta, M. R. Koblischka and M. Murakami, "High critical current densities in bulk MgB_2 fabricated using amorphous boron," *Phys. Status Solidi A*, vol. 212, no. 10, pp. 2141-2145, 2015.

[14] M. Takahashi, M. Okada, T. Nakane and H. Kumakura, "The influence of magnesium grain size and ball milling time on the phase formation of MgB_2 tapes," *Supercond. Sci. Technol*., vol. 22, pp. 125017, 2009.

[15] A. Martinelli, C. Tarantini, E. Lehmann, P. Manfrinetti, A. Palenzona, I. Pallecchi, M. Putti and C. Ferdeghini, "Direct TEM observation of nanometric-sized defects in neutron-irradiated MgB_2 bulk and their effect on pinning mechanisms," *Supercond. Sci. Technol*., vol. 21, pp. 012001, 2008.

[16] A. Matsumoto, H. Kumakura, H. Kitaguchi and H. Hatakeyama, "Effect of SiO_2 and SiC doping on the powder-in-tube processed MgB_2 tapes," *Supercond. Sci. Technol*., vol. 16, pp. 926-930, 2003.

[17] A. Yamamoto, J. Shimoyama, S. Ueda, I. Iwayama, S. Horii and K. Kishio, "Effects of B_4C doping on critical current properties of MgB_2 superconductor," *Supercond. Sci. Technol*., vol. 18, pp. 1323-1328, 2005.

[18] R. Zeng, S. X. Dou, L. Lu, W. X. Li, C. K. Poh, J. H. Kim, J. Horvat, D. Q. Shi, J. L. Wang, P. Munroe, X. F. Wang, R. K. Zheng, S. P. Ringer, M. Rindfleisch and M. Tomsic, "Stress/strain induced flux pinning in highly dense MgB_2 bulks," *IEEE Trans. Appl. Supercond*., vol. 19, pp. 2722-2725, 2009.

[19] B. -H. Jun, N. -K. Kim, K. S. Tan and C. -J. Kim, "Enhanced critical current properties of *in situ* processed MgB_2 wires using milled boron powder and low temperature solid-state reaction," *J. Alloys compd.*, vol. 492, pp. 446-451, 2010.

[20] S. Sugino, A. Yamamoto, J. Shimoyama and K. Kishio, "Enhanced trapped field in MgB_2 bulk magnets by tuning grain boundary pinning through milling," *Supercond. Sci. Technol*., vol. 28, pp. 055016, 2015.

[21] B. -H. Jun, S. -D. Park and C. -J. Kim, "Refinement and carbon incorporation effects on the superconducting properties of MgB_2 through wet milling process of low purity boron powder," *J. Alloys compd.*, vol. 535, pp. 27-32, 2012.

[22] A. Kikuchi, Y. Yoshida, Y. Iijima, N. Banno, T. Takeuchi and K. Inoue, "The synthesis of MgB_2 superconductor using Mg_2Cu as a starting material," *Supercond. Sci. Technol*., vol. 17, pp. 781-785, 2004.

[23] C. P. Bean, "Magnetization of high-field superconductors," *Rev. Mod. Phys.*, pp. 31-39, 1964.

[24] Á. Révész, T. Ungár, A. Borbély and J. Lendvai, "Dislocations and grain size in ball-milled iron powder," *Nanostruct. Mater*., vol. 7, pp. 779-788, 1996.

[25] D. N. Kim, B. -H. Jun, S. -D. Park, C. -J. Kim and H. W. Park, "Effects of the size of Mg powder on the formation of MgB_2 and the superconducting properties," *Prog. Supercond. Cryo*., Korea, vol. 18, no. 4, pp. 9-14, 2016.

[26] J. H. Yi, K. T. Kim, B. -H. Jun, J. M. Sohn, B. G. Kim, J. Joo and C. -J. Kim, "Pore formation in *in situ* processed MgB_2 superconductors," *Physica C*, vol. 469, pp. 1192-1195, 2009.

[27] J. H. Kim, S. X. Dou, J. L. Wang, D. Q. Shi, X. Xu, M. S. A. Hossain, W. K. Yeoh, S. Choi and T. Kiyoshi, "The effects of sintering temperature on superconductivity in MgB_2/Fe wires," *Supercond. Sci. Technol*., vol. 20, pp. 448-451, 2007.

[28] J. H. Kim, S. X. Dou, D. Q. Shi, M. Rindfleisch and M. Tomsic, "Study of MgO formation and structural defects in *in situ* processed MgB_2/Fe wires," *Supercond. Sci. Technol*., vol. 20, pp. 1026-1031, 2007.

[29] S. K. Chen, B. A. Glowacki, J. L. MacManus-Driscoll, M. E. Vickers and M. Majoros, "Influence of *in situ* and *ex situ* ZrO_2 addition on the properties of MgB_2," *Supercond. Sci. Technol*., vol. 17, pp. 243-248, 2004.

[30] Y. Chen, J. F. Gerald, J. S. Williams and S. Bulcock, "Synthesis of boron nitride nanotubes at low temperatures using reactive ball milling," *Chem. Phys. Lett*., vol. 299, pp. 260-264, 1999.

[31] P. Scherrer, "Bestimmung der grösse und der inneren struktur von kolloidteilchen mittels röntgenstrahlen," *Nachr. Ges. Wiss. Göttingen*, vol. 26, pp 98-100, 1918.